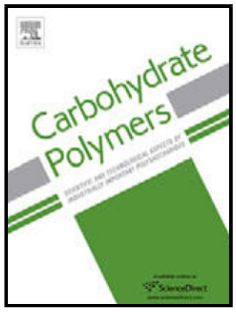

Title: Cellulose-pectin composite hydrogels: intermolecular interactions and material properties depend on order of assembly

Authors: Patricia Lopez-Sanchez, Marta Martinez-Sanz, Mauricio R. Bonilla, Dongjie Wang, Elliot P. Gilbert, Jason. R. Stokes, Michael. J. Gidley

PII: S0144-8617(17)30060-7
DOI: http://dx.doi.org/doi:10.1016/j.carbpol.2017.01.049
Reference: CARP 11927

To appear in:

Received date: 16-10-2016
Revised date: 27-12-2016
Accepted date: 13-1-2017

Please cite this article as: Lopez-Sanchez, Patricia., Martinez-Sanz, Marta., Bonilla, Mauricio R., Wang, Dongjie., Gilbert, Elliot P., Stokes, Jason R., & Gidley, Michael.J., Cellulose-pectin composite hydrogels: intermolecular interactions and material properties depend on order of assembly.*Carbohydrate Polymers* http://dx.doi.org/10.1016/j.carbpol.2017.01.049

Title:

Cellulose-pectin composite hydrogels: intermolecular interactions and material properties depend on order of assembly

Authors:

Patricia Lopez-Sanchez[1,a]*, Marta Martinez-Sanz[1,2], Mauricio R. Bonilla[3], Dongjie Wang[1], Elliot P. Gilbert[2], Jason. R. Stokes[3], Michael. J. Gidley[1]

Affiliations:

[1] ARC Centre of Excellence in Plant Cell Walls, Centre for Nutrition and Food Sciences, Queensland Alliance for Agriculture and Food Innovation, The University of Queensland, Brisbane, 4072, Australia

[2] Australian Centre for Neutron Scattering, Australian Nuclear Science and Technology Organisation, Locked Bag 2001, Kirrawee DC, New South Wales, 2232, Australia.

[3] School of Chemical Engineering, The University of Queensland, Brisbane, 4072, Australia

[a] Present address: Maurten AB. Biotech Center Arvid Wallgrens backe 20, SE-413 46 Gothenburg, Sweden.

*Corresponding author

Highlights:

- Cellulose-pectin-calcium gels were produced varying order of assembly and pectin DE
- Cellulose-pectin interactions occurred only when pectin was present during cellulose synthesis
- Order of polysaccharide assembly impacted hydrogels microstructure and mechanical properties
- The contribution to mechanical and diffusion properties depended on pectin DE
- These results highlight the multiple roles that pectin might have in cell wall mechanics

Abstract

Plant cell walls have a unique combination of strength and flexibility however, further investigations are required to understand how those properties arise from the assembly of the relevant biopolymers. Recent studies indicate that Ca^{2+}-pectates can act as load-bearing components in cell walls. To investigate this proposed role of pectins, bioinspired wall models were synthesised based on bacterial cellulose containing pectin-calcium gels by varying the order of assembly of cellulose/pectin networks, pectin degree of methylesterification and calcium concentration. Hydrogels in which pectin-calcium assembly occurred prior to cellulose synthesis showed evidence for direct cellulose/pectin interactions from small-angle scattering (SAXS and SANS), had the densest networks and the lowest normal stress. The strength of the pectin-calcium gel affected cellulose structure, crystallinity and material properties. The results highlight the importance of the order of assembly on the properties of cellulose composite networks and support the role of pectin in the mechanics of cell walls.

Keywords:

Cellulose, pectin, mechanics, XRD, SANS, SAXS

Introduction

Pectin is one of the main components of the primary cell wall of most plants; it is present in cells during growth and development and between adjacent cells (middle lamella). Furthermore, pectin is also present in the secondary walls of cells in woody tissues. Pectin's

functions are not only limited to cell structure, they have been found to play a role in plant growth and development, morphogenesis, cell–cell adhesion, signaling, wall porosity, and fruit development among others. The interaction of pectins with other cell wall polysaccharides and their influence on wall mechanics are not fully understood. Pectins are complex polymers which consist mainly of homogalacturonan (HG), rhamnogalacturonan I (RGI) and rhamnogalacturonan II (RGII) blocks covalently linked to one another (Atmodjo, Hao & Mohnen, 2013). HG is negatively charged, consisting of α-1,4-linked galacturonic acid (GalA) monomers that are partially methyl-esterified at the C-O-6 carboxyl. Interactions with calcium and other multivalent cations that lead to pectin gelation depend on the degree of methylesterification (DE) and the distribution of ester groups in homogalacturonan regions (Gidley, Morris, Murray, Powell & Rees, 1979; Peaucelle, Braybrook & Hofte, 2012; Strom, Ribelles, Lundin , Norton, Morris & Williams, 2007). Low methoxy pectins (DE < 50%) can form networks in the presence of divalent ions such as calcium. High methoxy pectins (DE > 50%) can also gel in the presence of calcium ions, depending on the distribution of the ester groups, although their gel strength is lower than for low DE pectins (Strom, Ribelles, Lundin , Norton, Morris & Williams, 2007).

In the most common representation of the primary plant cell wall of growing plants, pectin is depicted as an independent network, embedded in a load-bearing cellulose-hemicellulose network, with some structural proteins (Somerville et al., 2004). To date the major hemicellulose thought to be implicated in this network has been xyloglucan (XG). An increasing number of *in vitro* (Lin, Lopez-Sanchez & Gidley, 2015; Lin, Lopez-Sanchez & Gidley, 2016; Zykwinska et al., 2007) and *in muro* (Wang, Park, Cosgrove & Hong, 2015; Wang, Zabotina & Hong, 2012) studies suggest that pectin is not only present as an independent network but can also be in close contact with cellulose, through interactions with e.g. calcium-deficient regions of homogalacturonan (Lin, Lopez-Sanchez & Gidley, 2016)

and/or the arabinan and galactan sidechains characteristic of rhamnogalacturonan I (Lin, Lopez-Sanchez & Gidley, 2015; Zykwinska et al., 2007). In addition, studies on mutant plants (*xxt1/xxt2*; xylosyltransferase 1/2) (Park & Cosgrove, 2012) and tomato cell cultures (Shedletzky, Shmuel, Trainin, Kalman & Delmer, 1992) lacking XG, suggest that Ca^{2+}-pectate could presumably have a load bearing role in the absence of a cellulose-XG network (Peaucelle, Braybrook & Hofte, 2012).

Studying the role of individual biopolymers on cell wall properties *in planta* is challenging, due to the heterogeneity of plant tissues/organs and the ability of plants to adapt in response to environmental stimuli and compensate for changes in their genetic code. Therefore, hydrogels based on bacterial cellulose have been used as a tool for studies of plant cell wall assembly and to investigate the role of polysaccharides in cell wall mechanics (Chanliaud, Burrows, Jeronimidis & Gidley, 2002; Lopez-Sanchez, Rincon, Wang, Brulhart, Stokes & Gidley, 2014; Whitney, Brigham, Darke, Reid & Gidley, 1995). We have recently demonstrated that pectins contribute to the mechanical properties of these types of cellulose networks when they are present as a solution, in the absence of Ca^{2+}, through poroelastic effects (Lopez-Sanchez et al., 2016). Furthermore poroelasticity has been demonstrated for plant tissues *in vivo* in the work of Skotheim *et al*. (Skotheim & Mahadevan, 2005) however, its contribution to plant cell wall mechanics has not been investigated.

Here we demonstrate the diverse roles that pectin has on the micro- and nano-structure as well as on the mechanical properties of cellulose networks synthesised by the bacterium *Komagataeibacter xylinus* as a function of order of assembly of the pectin-calcium gel (either before or after cellulose deposition by *K. xylinus*), pectin degree of methylesterification and calcium concentration. The compression and relaxation behaviour is explained by a poroleastic model, and the effect of pectin-calcium gel presence during cellulose synthesis on cellulose architecture at different length scales is studied using X-ray diffraction (XRD),

small angle X-ray and neutron scattering (SAXS, SANS), scanning electron microscopy (SEM) and fluorescence recovery after photobleaching in combination with confocal laser scanning microscopy (FRAP-CSLM). Our results provide a better understanding of the multiple roles of pectin on cellulose networks with implications for cell wall mechanics and the biological control of wall properties at different stages of plant growth and development.

Materials and Methods

Production of cellulose-pectin hydrogels with Ca^{2+}-pectate gel assembly prior to cellulose synthesis

Pure cellulose hydrogels (C) were produced following the method described by Chanliaud *et al*. (Chanliaud & Gidley, 1999) In brief the *Komagataeibacter xylinus* (formerly *Gluconacetobacter xylinus*) strain ATCC 53524 (Manassas, VA, USA) was cultivated in Hestrin and Schramm medium (HS) at pH 5 with a glucose concentration of 2 % w/v. Two types of pectin were studied: (i) a high methoxy pectin DE 68-76 (Pectin CJ205, citrus, Herbstreith & Fox KG, Neuenbürg/Württ, Germany containing 71.1 % pectin with a composition of 85.9 % uronic acids, 10.7 % galactose (Gal), 3. 1 % arabinose (Ara) and 0.3 % xylose (Xyl); this material also contained 28.9 % glucose (Glu) which was added by the supplier and represented 7 % more glucose in the fermentation medium and, (ii) a low methoxy pectin DE 30 (Pectin AU-L 050/13, apple, Herbstreith & Fox KG , Neuenbürg/Württ, Germany with composition: 77.5 % uronic acid, 18.2 % galactose, 1.7 % xylose and 2.7 % glucose (Glu). Prior to inoculation, pectin and $CaCl_2$ solutions were added to the HS incubation medium. The pectin final concentration was 0.5 % w/v; the concentration of $CaCl_2$ was 2.5 mM for the low DE pectin and 6 mM $CaCl_2$ for the high DE pectin. These samples are referred to as CP low DE pre-gel and CP high DE pre-gel. We also included a sample produced in a 0.5 % w/v low DE pectin and a calcium content of 12.5 mM,

to evaluate the effect of having a higher amount of calcium present during synthesis; this sample will be referred to as CP low DE strong pre-gel.

All samples were cultivated statically at 30°C for 96 hours in 40 mm diameter containers. Pure cellulose hydrogels were washed 6 times with ice-cold water under agitation at 100 rpm to remove bacterial material and stored in 0.02 % NaN_3 solution. All CP hydrogels were washed with 12.5 mM $CaCl_2$ instead of water, and kept in 12.5 mM $CaCl_2$ solution containing 0.02 % NaN_3 in order to prevent leaching of pectin due to changes in the ionic environment. All composites were kept at 4°C until further analysis.

Production of cellulose-pectin hydrogels with Ca^{2+}-pectate gel assembly after cellulose synthesis

Pure cellulose hydrogels, synthesised as described above, were kept in 0.5 % high DE or low DE pectin solution at room temperature overnight. Samples were collected and their surface was sprayed with 2.5 mM or 6 mM $CaCl_2$ solution, for the low and high DE pectin respectively, following the method of Schuster *et al*. (Schuster et al., 2014). For the low DE pectin, a thin gel layer was immediately observed on the surface of the cellulose. 10 ml of 12.5 mM $CaCl_2$ was then added on top of the hydrogel and left in contact with the sample for two days at room temperature. The samples were then kept in 12.5 mM $CaCl_2$ with 0.02 % NaN_3 and stored at 4°C. These samples are referred to as CP high DE post-gel and CP low DE post-gel.

Pectin depletion by EDTA washing

Pectin depletion from the hydrogels was achieved by chelating the Ca^{2+} using excess 40 mM ethylenediaminetetraacetic acid (EDTA) with gentle agitation at room temperature for 24 hours. Extracted materials were removed three times during washing.

Chemical composition

Monosaccharide analysis

Chemical composition was calculated from individual sugar contents on the basis of dry weights following the method by Pettolino *et al.* (Pettolino, Walsh, Fincher & Bacic, 2012) with modifications as described in (Lopez-Sanchez et al., 2016), and analysed by GC-MS using a high polarity BPX70 column.

Uronic acid assay

Total uronic acid content was measured following a modification of the method by Filisetti-Cozzi *et al*. (Filisetti-Cozzi & Carpita, 1991) as described in reference (Lopez-Sanchez et al., 2016).

Calcium analysis

Calcium was analysed by inductively coupled plasma optical emission spectroscopy (ICP-OES). Samples were rinsed with deionised water prior to digestion to remove any calcium present in the samples not bound to pectin. Approximately 400 mg of sample was weighed and mixed with 6 ml of concentrated nitric acid and 2 ml of concentrated hydrochloric acid. Samples were pre-digested for 20 minutes at room temperature, subsequently 10 ml of triple deionised water (TDI) was added to each sample. Samples were digested for 20 min in a microwave digestor (Ethos-1, Milestone S.r.L, Bergamo, Italy). Digested and cooled samples were diluted with TDI water to a final volume of 25 ml. Samples were analysed using an ICP-OES instrument (Vista Pro,Varian, Melbourne, Australia) at 1200 W forward power. Sample introduction was done with a 2.0 ml/min Seaspray nebuliser and a Tracey spray chamber (Glass Expansion, Melbourne, Australia). Three replicate three-second integration readings were taken.

Dry weight

The total polysaccharide content was measured by drying the samples in an oven at 105°C for 24 h. The sample weight was measured before and after drying. Each sample was measured in duplicate.

Scanning electron microscopy (SEM)

Samples were prepared using a critical point dryer (Autosamdri-815, Tousimis, Rockville, Maryland 20852, USA) following a series of dehydration steps as described in reference (Lopez-Sanchez et al., 2016) and, examined in a JSM 7100 F scanning electron microscope (JEOL, Tokyo, Japan) at 5 kV and 10 mm working distance. Images were taken from at least three different locations of each sample and 6 images were taken from each position. All images were taken from the top side of the sample which is the one in contact with air during cellulose production.

X-ray diffraction (XRD)

The crystalline structure of the hydrogels was investigated by XRD measurements performed with a PANalytical X'Pert Pro diffractometer, according to the method described by Martinez-Sanz *et al.* (Martinez-Sanz, Lopez-Sanchez, Gidley & Gilbert, 2015). Peak fitting, crystallinity index and crystallite size determination were performed as described previously (Martinez-Sanz, Lopez-Sanchez, Gidley & Gilbert, 2015).

Small angle X-ray and neutron scattering (SAXS and SANS)

SAXS measurements, according to the method described by Martinez-Sanz *et al*. (Martinez-Sanz, Lopez-Sanchez, Gidley & Gilbert, 2015), were performed on a Bruker Nanostar.

SANS measurements were performed on the 40 m QUOKKA instrument at the OPAL reactor (Gilbert, Schulz & Noakes, 2006), following the experimental procedure described in (Lopez-Sanchez et al., 2016). The SANS data of the pure and composite hydrogels were fitted using the Igor NIST analysis macro suite (Kline, 2006) and applying the core-shell model described previously (Martinez-Sanz, Gidley & Gilbert, 2015). A detailed description of the form factor function and the parameters defining the model can be found elsewhere (Martinez-Sanz, Gidley & Gilbert, 2015).

Fluorescence recovery after photobleaching in combination with confocal scanning laser microscopy (CSLM-FRAP)

Fluorescein isothiocyanate labelled dextran (FITC-dextran) of two different molecular weights 70 000 (FD 70) and 500 000 (FD 500) g mol^{-1} (Sigma-Aldrich Pty. Ltd. Sydney, Australia) were selected based on previous results, which showed that both probes are suitable to characterise cellulose hydrogels (Lopez-Sanchez, Schuster, Wang, Gidley & Strom, 2015). Each diffusion probe was dissolved in deionized water to yield 500 ppm solutions. The hydrodynamic radius r_H and free diffusion coefficients D_0 of the probes in the absence of cellulose hydrogels were previously determined (Lopez-Sanchez, Schuster, Wang, Gidley & Strom, 2015), being 8.0 ± 0.5 nm and 30 ± 1.8 $\mu m^2\ s^{-1}$ for FD 70 and 13.5 ± 1.1 nm and 17.8 ± 1.04 $\mu m^2 s^{-1}$ for FD 500.

Hydrogels were immersed in 10 ml of 500 ppm FITC-dextran solution, the containers were covered with aluminium foil and left overnight at 5°C to give enough time for the probes to be homogeneously distributed in the samples. An approximately 2 cm x 2 cm sized sample was cut; the surface that was in direct contact with the liquid medium during cellulose synthesis was absorbed on a cover glass slid, then loaded on the microscope stage with FRAP measurements carried out at ambient temperature.

The CLSM system used consists of an LSM 700 Zeiss microscope (Jena, Germany) utilizing a 20 x, 0.8 numerical aperture objective, with the following settings: 200 x 200 pixels, zoom factor 4, yielding a pixel size of 0.41 μm. The 488 nm line of an argon laser was used to excite the fluorescent probes. FRAP experiments were conducted with a disk region of interest (ROI) of 30 μm diameter. The measurement routine consisted of 3 pre-bleach images, bleaching (laser at 100%) and post-bleaching (acquisition of images until the ROI intensity was constant). At least 3 FRAP measurements were performed on different spatial coordinates per sample. Each sample was measured in duplicate. We have previously

demonstrated (Lopez-Sanchez, Schuster, Wang, Gidley & Strom, 2015) that dextran probes do not interact with cellulose hydrogels and therefore diffusion of the probe occurs with no binding interaction between the probe and the sample. In the absence of interactions, a simple exponential equation can be used to fit the fluorescence recovery data

$$I(t) = I_{\infty}(1 - e^{\tau t}) \quad (3)$$

where I_{∞} is the final intensity in the ROI following recovery and τ is the recovery time constant.

FRAP analysis was performed within the ROI using the FRAP module in the Zen software (Zeiss, Germany). A recovery curve was plotted and normalized by taking into account the intensities immediately after bleaching and at the end of the experiment.

Viscoelasticity measurements of Ca^{2+}-pectate gels

The viscoelasticity of pectin-calcium gels (low and high DE) was assessed using a stress controlled rheometer TA 1500 (TA instruments, Delaware, USA) with concentric cylinders. An oscillatory test at 0.5% strain and 0.016 rad/s (1 Hz) was performed to determine the elastic and viscous moduli of pectin gels. Pectin solution (0.5% w:v) was loaded in the rheometer cup and warm 12.5 mM $CaCl_2$ was added whilst gently stirring for 15 s at 10 s^{-1}. Cure curves were recorded for 2 hours (Clark & Farrer, 1996). After this time, pectin gelation did not reach a final plateau therefore the gel values are considered only as estimates of the strength of the Ca^{2+}-pectate gels.

Mechanical testing and oscillatory rheology

Measurements were carried out on a rotational rheometer (HAAKE Mars III Rheometer, Thermo Fisher Scientific, Karlsruhe, Germany) at a temperature of 25°C, and an attached 60 mm diameter plate (calibrated for 40 mm diameter samples) coated with sand paper to reduce

sample slip during measurements. Hydrogel membranes were placed in the center of the bottom plate in the rheometer and, for each experiment, the gap was adjusted according to the sample thickness. Samples were compressed to the same initial cellulose concentration of 2% (w/w), calculated as previously described (Lopez-Sanchez, Rincon, Wang, Brulhart, Stokes & Gidley, 2014). Axial compression was applied on 2% cellulose samples at a constant speed of 1 μm/s for 100 μm whilst measuring the normal force. After the compression step, the relaxation of the normal force was followed simultaneously with a small amplitude oscillatory deformation test carried out for 180 s at a frequency of 0.016 rad/s (1 Hz) and at a constant stress of 1 Pa, chosen from the linear viscoelastic regime. The zero normal force was set for a gap where the upper plate was in close contact with the top surface of the samples. For each type of hydrogel at least three samples were measured.

Poroelastic model

The presence of a pectin gel induces a viscoelastic response that is not associated with the poroelastic effects characteristic of cellulose hydrogels (Lopez-Sanchez, Rincon, Wang, Brulhart, Stokes & Gidley, 2014). Therefore, an additional viscoelastic relaxation time is required to adequately capture the data. Since incorporating viscoelasticity in both radial and axial directions would introduce a number of parameters that cannot be unambiguously determined with a single test, viscoelasticity is incorporated in the axial direction only by linearly adding a Maxwell-like branch to the poroelastic stress $\sigma_{poro}(t)$:

$$\sigma_z(t) = \sigma_{poro}(t) + E_v\dot{\epsilon}\tau\left(1 - e^{-\frac{t}{\tau}}\right) \qquad for\ t < t_0 \tag{4}$$

and

$$\sigma_z(t) = \sigma_{poro}(t) + E_v\dot{\epsilon}\tau\left(e^{-\frac{t-t_0}{\tau}} - e^{-\frac{t}{\tau}}\right) \qquad for\ t \geq t_0 \tag{5}$$

where E_v is an effective viscoelastic modulus, $\dot{\epsilon}$ is the constant strain rate and τ the viscoelastic relaxation time. σ_{poro} is calculated as described in previous work (Bonilla, Lopez-Sanchez, Gidley & Stokes, 2016).

Results and Discussion

Composition of cellulose-pectin hydrogels containing Ca^{2+}-pectate gels

The chemical composition of all hydrogels produced in the presence of pectin was analysed after carefully removing a top loose pectin gel layer which did not contain cellulose, to ensure that pectin-calcium gels were incorporated within the cellulose hydrogels. The top loose layer was removed with tweezers and scalpel and the remaining solid material was used for chemical, structural and mechanical studies. Chemical analysis revealed that the main component of the removed top loose layer was uronic acid arising from calcium gelation of pectin coating the surface of the cellulose hydrogels.

Interestingly, the order of assembly of Ca^{2+}-pectate gel into the cellulose networks did not affect the incorporation level of pectin in the composite hydrogels (Table 1). However, pectin incorporation level did depend on pectin type. Pectin content was higher for the low DE pectin samples (35.7 % and 36.3 % for pre- and post-gel respectively) compared to the high DE pectin samples (18.1 % and 19.5 % for pre- and post-gel respectively). It has been previously shown (Chanliaud & Gidley, 1999) that the incorporation of Ca^{2+}-pectate gels (prior to cellulose synthesis) into cellulose networks was higher for low DE pectin compared to high DE pectin and likely related to the different calcium responsiveness of low and high DE pectins.

The total polysaccharide concentration was larger for the pre-gels, especially in the case of the high DE pectin (Table 1); this indicates that the pre-gels held less water and were denser than the post-gels. Calcium incorporation was very similar in all samples 2-3 % (dry weight), confirming that it was possible to gel pectin by slow diffusion of calcium into the cellulose

hydrogels. Cellulose-pectin hydrogels produced in the presence of higher amounts of calcium (12.5 mM) were inhomogeneous and fragile; as a result, values for the pectin incorporation (17.7 % dry weight) should be interpreted with care since different parts of the sample will have different incorporation levels.

Table 1. Chemical composition and crystallinity of cellulose-pectin hydrogels before and after washing three times with 40 mM EDTA. *Pectin content is based on analysis of total uronic acids. (nd = not determined). All values correspond to the average of two independently hydrolysed samples. The standard variation for the total uronic acid test is ± 5 %. The standard variation for the concentration calculations is 0.1-0.3 %. Different letters in the same column denote significant differences. Crystallinity index (X_C) and cross-sectional dimensions of crystallite sizes in the direction perpendicular to the (100), (010) and (110) planes (D_{100}, D_{010} and D_{110}), were determined from the XRD patterns of air-dried samples.

Sample	Sample code	Total uronics* (% dry weight)	Total polysaccharide concentration (% wet weight)	Cellulose concentration (% wet weight)	Calcium (% dry weight)	X_C (%)	D_{100} (nm)	D_{010} (nm)	D_{110} (nm)
Cellulose	C	0	0.9[a]	0.9	nd	98.9	4.9	7.5	6.2
Cellulose produced in Ca^{2+}-pectate gel (low DE)	CP low DE pre-gel	35.7[a]	1.5[a,b]	1	1.9	92.1	4.4	6.6	5.7
Cellulose + post addition of Ca^{2+}-pectate gel (low DE)	CP low DE post-gel	36.3[a]	1.12[a]	0.7	2.0	98.8	4.6	7.0	6.1
Cellulose produced in Ca^{2+}-pectate gel (high DE)	CP high DE pre-gel	18.1[b]	1.8[b]	1.5	3.1	93.9	4.6	7.6	5.8
Cellulose + post addition of Ca^{2+}-pectate gel (high DE)	CP high DE post-gel	19.5[b]	0.71[a]	0.6	2.7	99.6	5.0	8.3	6.5
Cellulose produced in Ca^{2+} pectate strong gel (low DE)	CP low DE strong pre-gel	17.7[b]	1.9[b]	1.5	nd	88.0	4.6	6.9	5.7
Washed cellulose produced in Ca^{2+}-pectate gel (low DE)	Washed CP low DE pre-gel	6.8[c]	2.2[b]	2.0	nd	98.0	4.8	7.5	6.5
Washed cellulose + post addition of Ca^{2+}-pectate gel (low DE)	Washed CP low DE post-gel	3.7[c]	1.0[a]	0.9	nd	99.6	5.0	7.9	6.7

Washed cellulose produced in Ca^{2+}-pectate gel (high DE)	Washed CP high DE pre-gel	5[c]	1.1[a]	1	nd	95.9	4.7	7.0	6.0
Washed cellulose + post addition of Ca^{2+}-pectate gel (high DE)	Washed CP high DE post-gel	0.0[c]	1.3[a]	1.3	nd	99.7	4.9	9.7	6.7
Washed cellulose produced in Ca^{2+} pectate strong gel (low DE)	Washed CP low DE strong pre-gel	7.6[c]	nd	nd	nd	89.7	4.7	6.1	5.7

After calcium chelation using EDTA, most of the pectin (80-90 %) was removed from the low DE pectin samples. A small percentage of pectin remained, 6.8 % (dry weight) and 3.7 % for the pre- and post-gel respectively. For the high DE pectin samples, ca. 70 % pectin was removed from the pre-gel by EDTA washing (5 % dry weight remaining) and 100% was depleted from the post-gel. Thus a large fraction of pectin was easily removed from the pre-gels by calcium chelation and a minor fraction remained even after multiple EDTA washing. In the post-gels either all, or almost all, of the pectin was removed by washing the samples with EDTA (Table 1). Two pectin fractions have also been found in cellulose hydrogels produced in pectin solutions, in the absence of calcium (Lopez-Sanchez et al., 2016): a major fraction associated with (adsorbed to) cellulose surfaces, which was depleted by water washing, and a minor fraction that remained after water washing and that was able to interact with cellulose at the molecular level. The amount of bound pectin is related to both the pectin gelation mechanism and to the mechanism of cellulose-pectin interaction (which is limited to the surface of cellulose ribbons in the case of the post-gels).

Microstructure of cellulose-pectin hydrogels

All hydrogels were disk in shape with a diameter of 40 mm and 2-3 mm thickness. Figure 1 shows the microstructure of the cellulose-pectin hydrogels. Before washing, the cellulose ribbons appeared to be embedded in a dense pectin matrix (see Figure S1) in the low DE

samples. After washing with EDTA, the cellulose ribbons, with a diameter of 50-100 nm and random orientation, could be clearly detected. Although not detected in the SEM micrographs, the individual microfibrils in bacterial cellulose have been reported to present a diameter of ca. 5nm (Martinez-Sanz, Lopez-Sanchez, Gidley & Gilbert, 2015). Micrographs of washed low DE post-gels revealed a more open cellulose network than that of washed low DE pre-gels, suggesting a denser structure for the pre-gels, in agreement with the total polysaccharide concentration (Table 1). The microstructures of the cellulose-pectin hydrogels containing high DE pectin were qualitatively similar to the ones containing low DE pectin. The cellulose network of the post-gel sample, which could be observed after washing, was more open than for the pre-gel. Pre-gel samples showed denser cellulose networks, similar to the ones observed for low DE pectin samples and pure cellulose, consistent with compositional analysis (Table 1).

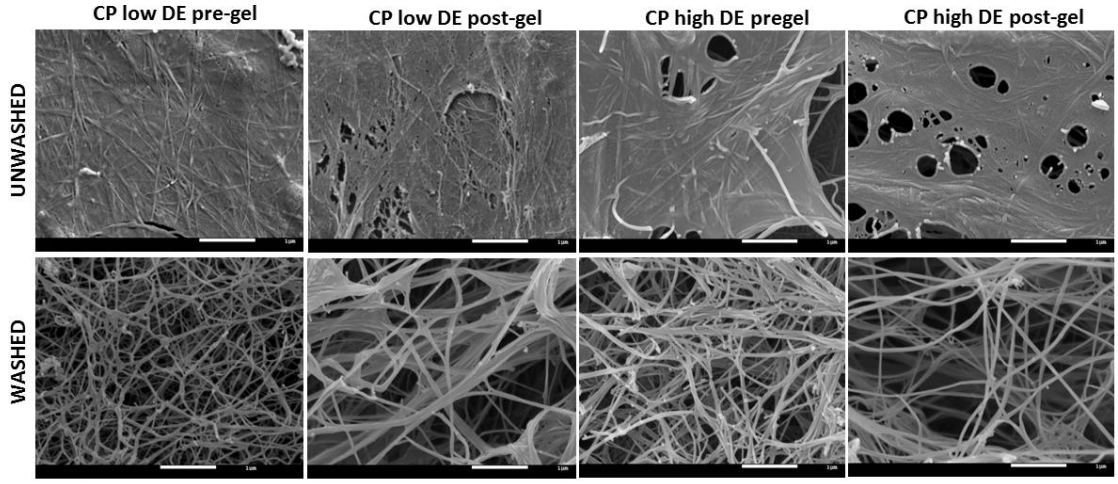

Figure 1. Scanning electron microscopy images of cellulose-pectin-calcium hydrogels with low and high DE pectins. Hydrogels were prepared by varying order of assembly. Cellulose was synthesised in the presence of pectin-calcium gels (pre-gel) or the pectin-calcium gel was

introduced after cellulose synthesis (post-gel). Top raw: unwashed hydrogels. Bottom raw: hydrogels after EDTA washing. Scale bar 1µm.

Samples produced in the presence of a higher $CaCl_2$ concentration were inhomogeneous and broke easily upon handling. Microscopic analysis revealed a heterogeneous structure in which patches of Ca^{2+}-pectate gels were aggregated in close proximity to the cellulose ribbons (Figure S1).

Crystalline configuration: XRD of air-dried composites

As observed in Figures 2A and 2B, the patterns from the cellulose-pectin hydrogels containing Ca^{2+}-pectate gels are quite similar to that of pure cellulose, presenting the three diffraction peaks characteristic of the cellulose I_α crystalline allomorph at 2θ values of 14.5°, 16.9° and 22.7° (corresponding to the (100), (010) and (110) crystalline planes, respectively). Although the position of the peaks is not affected by the incorporation of pectin, hence indicating that the I_α/I_β allomorph is not affected significantly, the relative intensity and the peak widths are modified. Table 1 summarises the crystallinity index and crystallite sizes estimated from peak fitting. The incorporation of pectin gels leads to a reduction in the crystallinity index and crystallite cross-section, this effect being more obvious for the low DE pectin and, in particular, for the CP low DE strong pre-gel. This effect (Table 1) is related to the strength of the Ca^{2+}-pectate gel, with stronger pectin gels having a greater effect on the cellulose crystallinity. The elastic modulus G' of the gels formed by low DE pectin and high DE pectin with 12.5mM $CaCl_2$ was measured as an indication of gel strength. It was found that the G' of the low DE pectin gel was 475 Pa and $\tan \delta = 0.11$, whilst the high DE pectin had a G' of 7.6 Pa and $\tan \delta = 0.22$. In agreement with this hypothesis, cellulose-pectin

hydrogels with the high DE pectin contained the weakest Ca^{2+}-pectate gels and had the least effect on cellulose crystallinity (Table 1).

It is interesting to note that the effect of pectin gels on crystallinity is significantly weaker than that previously reported for pectin solutions (Lopez-Sanchez et al., 2016). The diffraction pattern of pectin when prepared as a solution showed a broad amorphous halo centred at around 19.8° and a very weak peak at 15.8° (Lopez-Sanchez et al., 2016). In contrast, as shown in Figure 2A, the pectin gels, regardless of the amount of Ca^{2+}, present two weak amorphous halos centred at 12.1° and 22.5° and several small diffraction peaks located at 14.8°, 29.7° and 31.8°; this is indicative of the formation of a more ordered structure, as described by e.g. the egg-box model (Grant, Morris, Rees, Smith & Thom, 1973), when pectin is in the form of Ca^{2+}-pectate gels. The strong effect observed for the pectin solutions was attributed to a cellulose-pectin phase separation occurring when the samples were air-dried, with the non-interacting pectin excess migrating to the surface of the sample (Lopez-Sanchez et al., 2016). Such an effect would be limited in the case of the pectin gels, hence having a weaker effect on the shape of the diffraction patterns from the composite hydrogels.

After washing the hydrogels with EDTA, the samples show almost the same crystallinity and crystallite size as native pure cellulose, except for the sample synthesised in the presence of the largest concentration of $CaCl_2$, namely the CP low DE strong pre-gel. This indicates that although there is a small amount of pectin which remains in the samples after washing with EDTA, it does not have a significant effect on the cellulose crystalline structure. In the particular case of the CP low DE strong pre-gel, the high viscosity of the culture medium may have affected the cellulose assembly, hence leading to the formation of more defective cellulose microfibrils, i.e. with lower crystallinity.

None of the post-gel samples presented a significant effect on the cellulose crystallinity. This is unsurprising, since the addition of Ca^{2+}-pectate in these samples occurred after cellulose

synthesis and, therefore, is not expected to result in the establishment of strong interactions between pectin and the individual cellulose microfibrils.

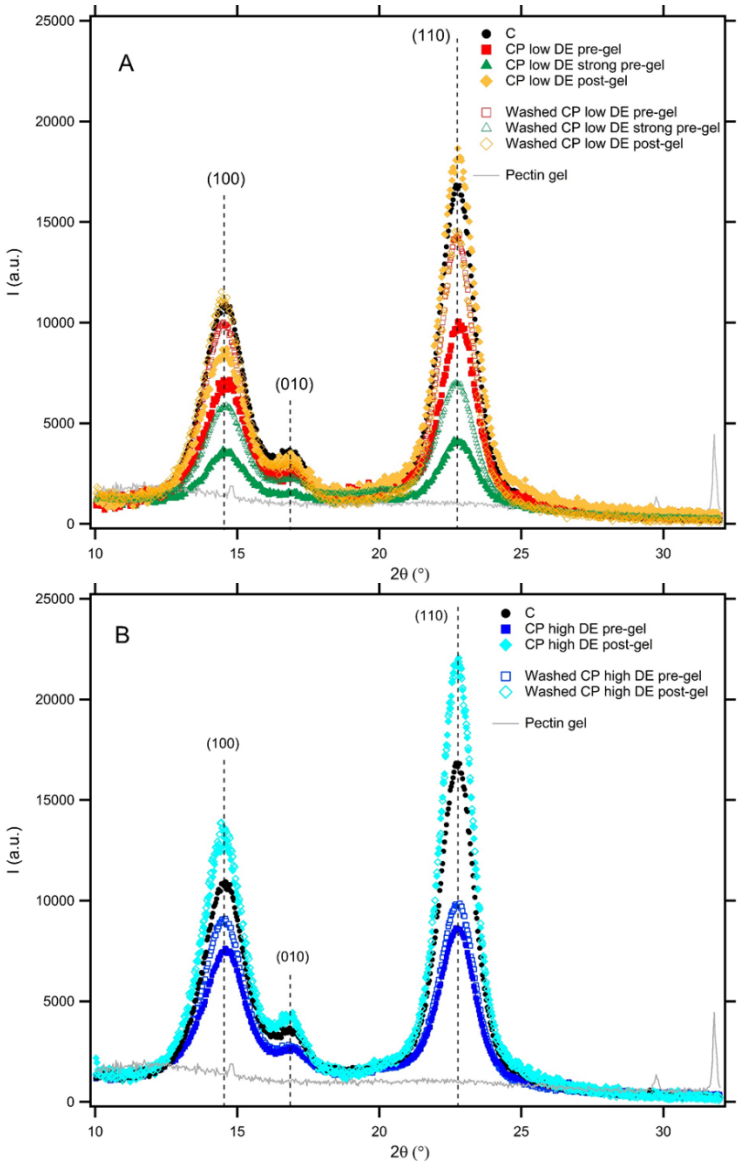

Figure 2. XRD patterns of pure cellulose hydrogels and cell wall models with Ca^{2+}-pectate gels before and after washing with EDTA (A) low DE pectin and (B) high DE pectin samples.

Small angle scattering (SAXS and SANS)

SAXS experiments showed, as a general trend, that the incorporation of pectin into the hydrogels led to a decrease in the intensity within the low q region (Figures 3A and 3B). Such an effect has been previously related to a decreased contrast in scattering length density

(SLD) due to the partial replacement of water by pectin between cellulose microfibrils and/or ribbons (Lopez-Sanchez et al., 2016) (see Table S1 for the SLD values of the different components forming the hydrogels). This would explain why the effect is more evident in the case of the low DE pre- and post-gels as compared with the high DE pectin gels, since the latter contain less pectin (Table 1). After EDTA washing, and removing most of the pectin, the scattering intensity remains constant or slightly decreases for most of the samples, but a significant increase in the intensity is observed for the CP low DE pre-gel. This effect is consistent with the increase in sample density (concentration) after washing (Table 1). Interestingly, the scattering pattern from the CP low DE strong pre-gel shows a small peak at ca. $q = 0.13$ $Å^{-1}$ (indicated by an arrow in Figure 3A), corresponding to a real distance of ca. 5 nm. This peak has been previously detected in the SAXS patterns of air-dried bacterial cellulose and has been attributed to the centre-to-centre distance between the crystalline cellulose microfibrils, which are closely packed together in the absence of moisture (Martinez-Sanz, Lopez-Sanchez, Gidley & Gilbert, 2015). This observation may be indicative of the cellulose microfibrils being more closely packed in this sample, confirming that a dense cellulose network structure arose in this case, most likely due to the presence of a robust pectin network, promoting cellulose self-interactions during the biosynthetic assembly process.

The SAXS patterns of the air-dried samples were also collected (Figure 3C). As expected, all the samples, except for the high DE post-gel, present the cellulose interfibrillar peak located at ca. $q = 0.13$ $Å^{-1}$, becoming more visible than for the pure cellulose, especially in the case of the CP low DE strong pre-gel. According to the peak position, intensity and width values estimated by fitting the scattering intensity within the q range of interest with a power-law plus Lorentzian peak function, the improved appearance of this peak is a consequence of the reduced interfacial scattering caused by the presence of pectin, except for the CP low DE

strong pre-gel. In that case, the creation of larger SLD contrast between crystalline and amorphous domains in this less crystalline sample might also be responsible for the appearance of a more intense interfibrillar peak. The scattering curve of pure cellulose and the high DE post-gel are almost identical but with reduced intensity for the latter due to the lower contrast in the presence of pectin, which could explain why the peak is not present in this sample. Additionally, all the pre-gels present a broad shoulder, similar to that previously detected for pectin solutions (Lopez-Sanchez et al., 2016), centred at ca. $0.07A^{-1}$, corresponding to a real distance of ca. 9 nm. These shoulders have been attributed to the pectin domains interacting with the individual cellulose microfibrils (Lopez-Sanchez et al., 2016). The fact that the shoulders are absent in the scattering patterns from the post-gels confirms that discrete cellulose-pectin interactions at the microfibril level are not established in this case.

Several important implications may be deduced from the SAXS results. First of all, the incorporation of Ca^{2+}-pectate gels into the hydrogels leads to the formation of denser networks. Secondly, and in agreement with the XRD results, pectin may be able to establish interactions with the individual cellulose microfibrils when incorporated into the culture medium (i.e. prior to assembly into mature ribbons), while only ribbon surface interactions can arise when the pectin gels are added after the cellulose has been synthesised. Furthermore, in the case of the pre-gels, the cellulose-pectin network structure created with the low DE and high DE pectins seems to be quite different: while cellulose recovers partially its hydration level upon removal of the high DE pectin gel, the opposite happens when removing the low DE pectin gel. This may be indicative of a collapse of the cellulose microfibrils when the pectin domains are removed in the latter case.

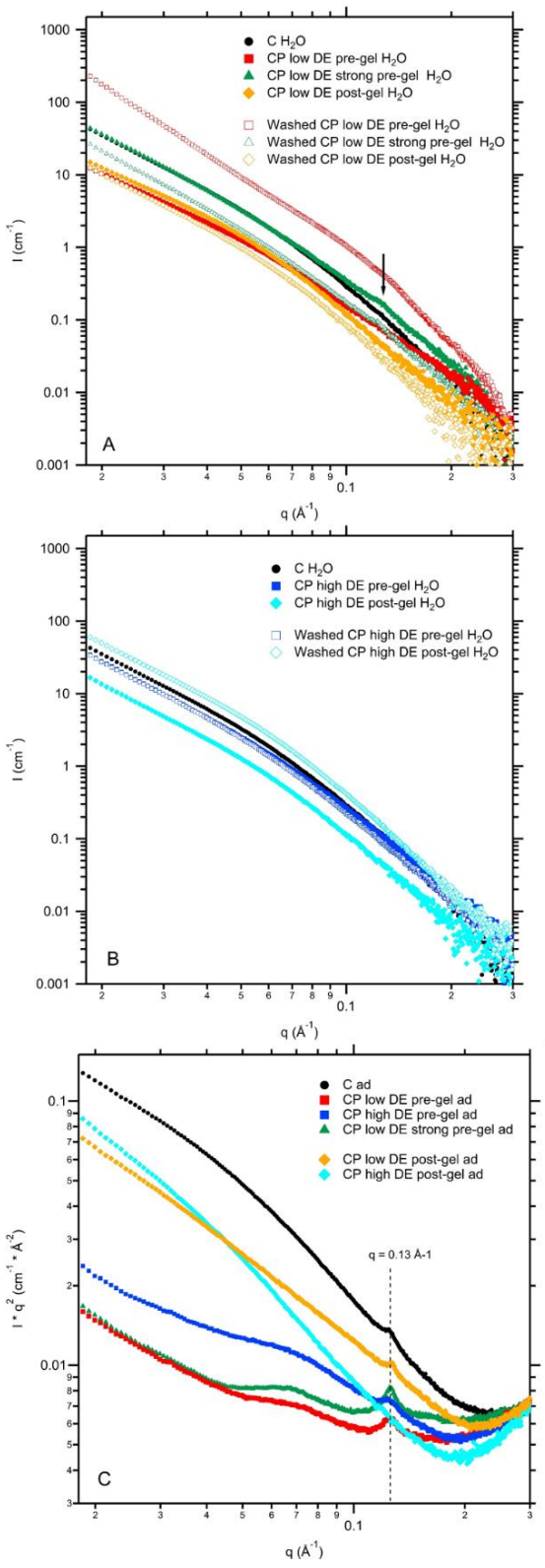

Figure 3. SAXS measurements from pure cellulose hydrogels and composites with Ca^{2+}-pectate gels in the hydrated state, before and after washing with EDTA. (A) Low DE pectin and (B) high DE samples. (C) SAXS Kratky plots from the corresponding air-dried samples.

In addition to the SAXS experiments, the hydrogels were characterised by SANS to probe the structure at the ribbon size range. As shown in Figure S2, while the 2-D SANS patterns of all the samples presented isotropic scattering, the CP low DE pre-gel, before and after washing with EDTA, showed slightly anisotropic behaviour. The scattering intensity in the equatorial and meridional directions was obtained by applying reduction procedures in which the data were sector-averaged and the so-obtained patterns are shown in Figure S3. The intensity in the equatorial direction is ca. 1.5-fold the intensity in the meridional direction over the whole q range. Hence, the anisotropy in these particular samples is related to the preferential orientation of the cellulose network structure along a certain direction, which is promoted by the presence of low DE Ca^{2+}-pectate in the culture medium and is maintained after most of the pectin has been removed.

The radially averaged data, displayed in Figures 4A and 4B, show the appearance of shoulder-like features which have been previously detected in the SANS patterns of pure cellulose hydrogels (Martinez-Sanz, Lopez-Sanchez, Gidley & Gilbert, 2015) and hydrogels containing pectin solutions (Lopez-Sanchez et al., 2016). As observed, the scattering intensity for most of the composite hydrogels decreases in comparison to the pure cellulose and in the particular case of the pre-gel samples, the shoulder features become more pronounced, especially with the low DE pectin. The decrease in the scattering intensity is likely to be a consequence of the denser network structure observed in the composite hydrogels. On the other hand, the more defined shoulders may arise from the presence of pectin coating the cellulose microfibrils, therefore affecting the properties of the ribbons' core.

The detected shoulder features have been assigned to the gradual exchange undergone by the cellulose ribbons when soaking the cellulose hydrogels in D_2O (Martinez-Sanz, Gidley &

Gilbert, 2015; Martinez-Sanz, Lopez-Sanchez, Gidley & Gilbert, 2015). According to a previously developed model, cellulose ribbons can be described as core-shell systems, containing a core composed of cellulose microfibrils (crystalline and paracrystalline domains) interacting with each other, and with bound solvent by means of hydrogen bonds and a more accessible shell composed of hydrated paracrystalline cellulose. The same core-shell cylinder plus power-law model previously used to fit the SANS data from different cellulose hydrogels (Martinez-Sanz, Gidley & Gilbert, 2015; Martinez-Sanz, Lopez-Sanchez, Gidley & Gilbert, 2015; Martinez-Sanz, Mikkelsen, Flanagan, Gidley & Gilbert, 2016) was applied to successfully fit the experimental data from the cellulose/Ca^{2+}-pectate hydrogels (Figures 4A and 4B). The associated fitting parameters (Table S2) indicate that the cellulose ribbon structure is affected for the hydrogels synthesised in the presence of pectin gels (i.e. pre-gels) and for the high DE pectin post-gel. Specifically, the overall ribbon cross-section increases from ca. 28 nm for the pure cellulose to ca. 33 nm for the CP low DE pre-gel and CP low DE strong pre-gel, ca. 32 nm for the CP high DE post-gel and ca. 36 nm for the CP high DE pre-gel. The (apparent) cellulose volume fraction within the core appears to decrease and the solvent H/D exchange increases with the incorporation of pectin into the system. According to the densification effect indicated from SAXS and SEM characterisation, the fitting results seem to indicate that the SLD within the ribbons' core increases due to the presence of pectin (see Table S1 for approximate values of the neutron SLD of pectin). On the other hand, the cellulose volume fraction within the ribbons' shell tends to increase with the addition of pectin, confirming the existence of less hydrated systems as already suggested by SAXS.
The fitting results suggest structural heterogeneity for the CP low DE post-gel and for all the samples after pectin depletion by washing with EDTA. This is demonstrated by the absence of characteristic shoulders in the corresponding SANS patterns and the large core radius

polydispersity values obtained. Such heterogeneity is in fact observed in the corresponding SEM images (Figure 1), where ribbon aggregates are detected after pectin depletion.

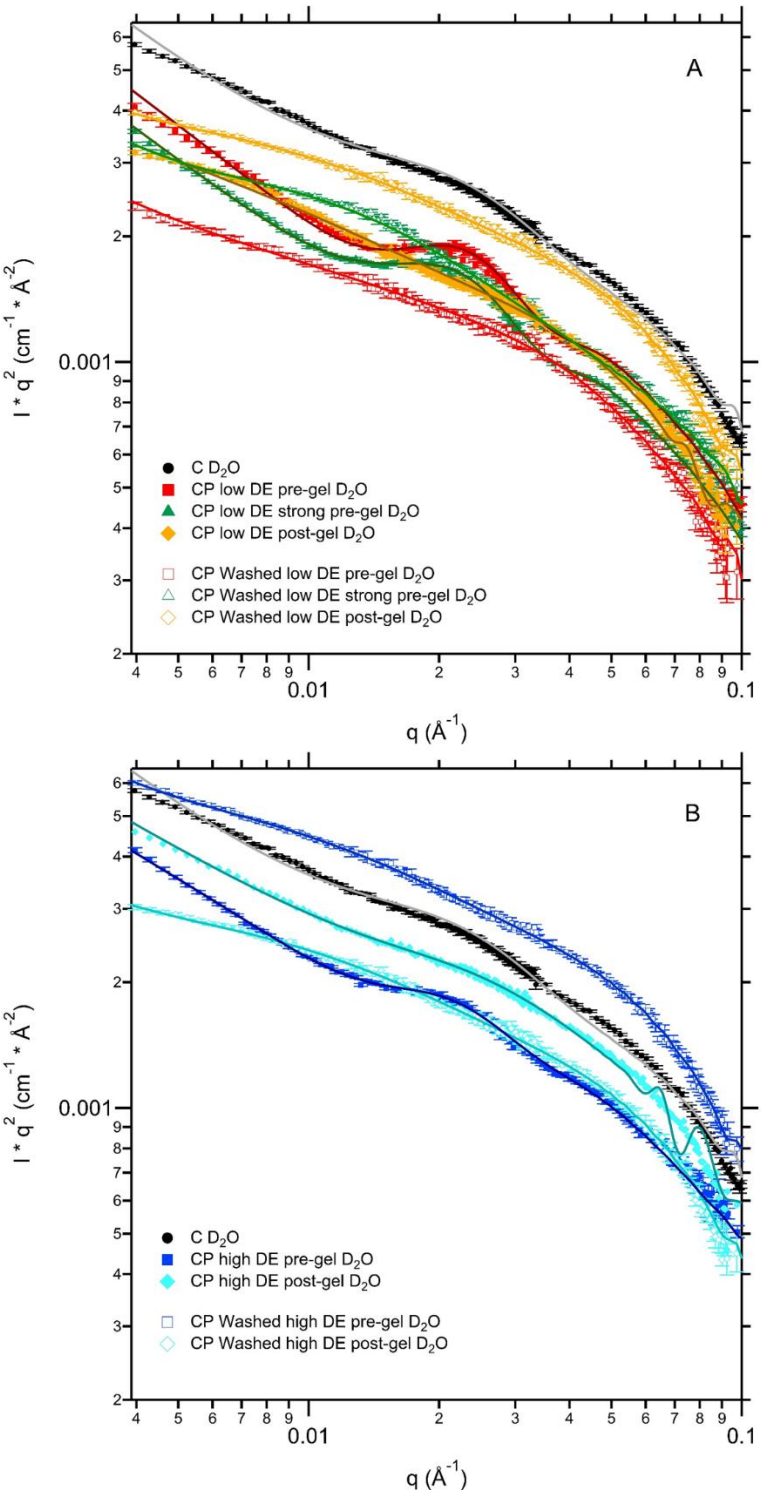

Figure 4. SANS Kratky plots from the pure cellulose and cellulose/Ca^{2+}-pectate gels (soaked in D_2O), before and after washing with EDTA. (A) Samples containing low DE pectin and

(B) high DE pectin. Solid lines correspond to the fitting of the experimental data using the core-shell model.

Mechanics and poroelastic behaviour: effects of order of assembly.

To evaluate the impact of having a second networked polymer in the cellulose structure on the mechanical properties, the samples were first concentrated to the same cellulose content (i.e. 2%, which corresponded to thicknesses of 1.3 ± 0.6 mm and 1.2 ± 0.3 mm for unwashed and washed samples respectively) by compression. We have previously shown that pure cellulose and cellulose-hemicellulose hydrogels have a near zero Poisson's ratio, which enables the cellulose concentration to be recalculated as the samples are compressed and liquid is released, whilst their diameter remains constant (Lopez-Sanchez, Rincon, Wang, Brulhart, Stokes & Gidley, 2014). As observed in Figure 5A, despite having similar pectin and calcium incorporation, the addition of Ca^{2+}-pectate gel after cellulose synthesis (CP low DE post-gel) led to higher normal stress, or higher load bearing ability, than when the pectin was present prior to cellulose synthesis (CP low DE pre -gel), 1166 Pa for the post-gel and 410 Pa for the pre-gel (Table 2). Both types of samples showed higher normal stress than pure cellulose with a value of 127 Pa, indicating than the presence of a Ca^{2+}-pectate gel increased the resistance to compression of these hydrogels. Removal of the pectin gel by calcium chelation using EDTA led to a decrease in normal stress; this demonstrates that the pectin gel itself contributes to resistance to compression. Washed pre-gels had higher normal stress that the washed post-gels, in agreement with the presence of denser cellulose networks in the pre-gels, as shown by scattering and microscopy data.

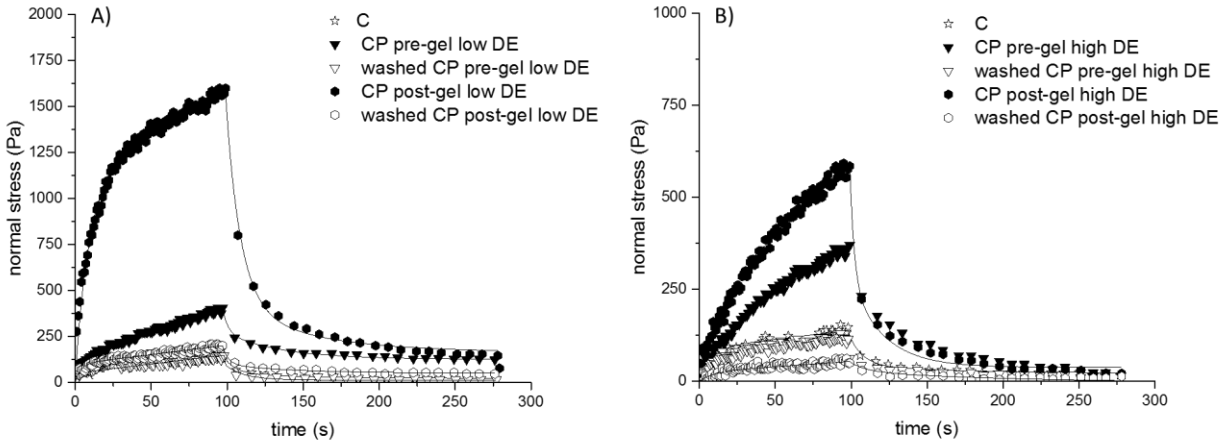

Figure 5. Compression-relaxation behaviour of hydrogels (2 % cellulose) containing Ca^{2+} pectate gel added prior to, or after, cellulose synthesis a) Low DE pectin and b) High DE pectin. Symbols represent experimental data. Solid lines represent fitting to a poroelastic model (Bonilla, Lopez-Sanchez, Gidley & Stokes, 2016).

It has been previously demonstrated that hydrated cellulose networks in pure and composite hydrogels containing hemicelluloses behave as poroelastic materials (Lopez-Sanchez, Rincon, Wang, Brulhart, Stokes & Gidley, 2014) (Lopez-Sanchez, Cersosimo, Wang, Flanagan, Stokes & Gidley, 2015). In this work, a modified poroelastic theory is used to explain and analyse the compression-stress relaxation. The poroelastic or biphasic theory predicts that, under unconfined compression, the fluid phase will contribute to the deformation generating a high internal pressure, depending on its viscosity and viscoelastic properties which, in turn, contributes to the normal stress and resistance to compression. A second interpenetrating, isotropic network with low porosity such as a pectin gel will reduce the permeability and increase the sample elasticity, while additionally introducing a second relaxation time due to its intrinsic viscoelasticity. This theory predicts the mechanical behaviour of materials which can be defined as porous soft systems filled with a fluid phase. Table 2 summarises the parameters obtained from the experiments and from fitting the data to

the poroelastic model. Applying the poroelastic theory, parameters are obtained such as the radial (E_r) and axial moduli (E_z), the equilibrium axial modulus (E_f) and an estimation of sample elasticity from E_f/E_z*100 (100 indicates totally elastic sample). All samples showed a radial modulus larger than the axial modulus, characteristic of samples which are strong radially, as observed for these cellulose hydrogels. However, pre-gels had lower moduli than post-gels suggesting that the presence of a pectin-calcium gel during cellulose synthesis led to overall weaker structures than when the pectin gels where assembled after cellulose production. The ratio E_f/E_z of the pre-gels was larger compared to that of the post-gels, indicating the more elastic nature of the pre-gels. Samples in which the pectin-calcium gels were present during cellulose deposition showed higher permeability than those with post addition of the pectin-calcium gels. Removal of Ca^{2+}-pectates by EDTA washing increased the ratio E_f/E_z of both pre- and post-gels, indicating that the pectin gel reduced hydrogel elasticity. Furthermore, the permeability of washed low DE pectin samples increased, suggesting that the pectin-calcium gel controlled sample permeability i.e. it was the component with the smallest mesh size. This change in permeability was less evident in the samples containing high DE pectin.

Although the chemical composition of the Ca^{2+}-pectate gel in pre- and post- gel cell wall models was very similar (Table 1), the microstructural analysis revealed that the cellulose network (at all length scales) was denser in the pre-gels or, in other words, they held less water. The differences in compression behaviour between pre- and post- gels could be due to the different distribution of the Ca^{2+}-pectate gels between assembly before or after cellulose synthesis. Assembly of the Ca^{2+}-pectate gel after cellulose synthesis is proposed to lead to a more homogeneous distribution of the gel, whilst synthesis of cellulose in the presence of the Ca^{2+}-pectate could generate heterogeneities in the microstructure which make it easier for the water to escape during compression, generating lower internal pressure. Pre-gels had less

water and a more heterogeneous structure; due to the poroelastic nature of these systems, these two parameters will lead to lower compression stress. In the post-gels, a more homogeneous pectin gel network may create a more tortuous path for the water to leave the system whilst, in the pre-gel samples, heterogeneities could lead to local aggregation of pectin gel and water channels enabling water to leave the system more readily. Indeed, this could be reflected in the different values of permeability k, post-gels have a lower k, for both low and high DE (Table 2).

Table 2. Experimental peak normal stress and parameters obtained from fitting experimental data to the poroelastic model (Bonilla, Lopez-Sanchez, Gidley & Stokes, 2016). Cellulose hydrogels (2% cellulose) containing Ca^{2+}-pectate gels of different degree of methyl esterification. Pectin gels were introduced before or after cellulose deposition. Pure cellulose is shown for comparison. E_r - radial modulus, E_z - instantaneous axial modulus, E_f - equilibrium axial modulus and k - permeability.

Sample	**Peak normal stress (Pa)**	**E_r (kPa)**	**E_z (kPa)**	**E_f (kPa)**	**E_f/E_z*100**	**k x 10^{-13} (m^2)**
C	127 ± 27	56.5	0.62	0.29	47.0	3.6
CP low DE pre-gel	410 ± 190	56.9	2.83	1.29	45.6	3.2
Washed CP low DE pre-gel	184 ± 37	26.2	5.48	4.77	87.2	11
CP low DE post-gel	1166 ± 381	113.8	4.83	1.83	37.9	0.3
Washed CP low DE post-gel	169 ± 43	19.1	1.34	0.68	50.3	3.2
CP high DE pre-gel	351 ± 82	65.4	2.68	1.18	47.3	3.1
Washed CP high DE pre-gel	115 ± 7.0	57.8	0.75	2.8	79	3.3
CP high DE post-gel	569 ± 21	154.8	3.35	0.66	19.8	1
Washed CP high DE post-gel	50 ± 16	32.9	0.69	0.14	20.4	1.3

Mechanical and poroelastic behaviour: effect of pectin degree of methylesterification.

Similar trends were observed for low and high DE pectins, although the samples containing low DE pectin gels showed larger compression stress than high DE pectin samples. This could be due to the differences in viscoelasticity and gel strength between the low and high

DE Ca^{2+}-pectate gels. The elastic modulus G' of the low DE pectin with 12.5mM $CaCl_2$ was 475 Pa and tan $\delta = 0.11$; for the same concentration of $CaCl_2$, the high DE pectin gel had a G' of 7.6 Pa and tan $\delta = 0.22$. These values are indicative of gel formation (G" < G') and the strength of the gels. High DE pectin led to a weaker gel than the low DE pectin, thus contributing less to the load-bearing properties of the cellulose composites due to their poroelastic nature. Furthermore, whilst high DE gels were able to completely relax during the time of the experiment, the samples containing low DE pectin gels did not relax completely, indicated by a residual stress at the end of the relaxation experiment (Figure 5).

Effect of pectin-calcium gels on the diffusion properties of cellulose hydrogels

Diffusion coefficients calculated from FRAP experiments are presented in Figure 6. As can be observed, diffusion depends more on probe size than on type of sample. There were no significant differences in the diffusion values of pre- and post-gels. However, the samples containing low DE pectin showed lower average diffusion values than the high DE samples, in particular for the probe with the smallest size. This could indicate that samples with low DE pectin/calcium gel had denser networks than the corresponding high DE samples, due to the different fine structure of the pectins and the corresponding gel networks. There is no correlation between these diffusion coefficients and the permeability values obtained from the poroelastic model, which showed that the pre-gels were more permeable than post-gels and both low and high DE samples had similar permeability. The lack of correlation could be due to the different length scales investigated; using FRAP, information on 30 μm diameter regions is obtained, whereas the poroelastic model used data from the whole experimental sample with a diameter of 40 mm and thickness of ca. 1mm. Furthermore, the diffusion values from FRAP correspond to 3D movement of the probes in the samples whilst the permeability from the poroelastic model is mainly in the radial direction. One can conclude

that whilst order of assembly impacts the diffusion properties of the cellulose/pectin/calcium composites at large length scales due to heterogeneities, it has no measurable impact at lower length scales. However, pectin degree of methylesterification has an effect on the diffusion at lower length scales, due to the differences in fine structure and gel network.

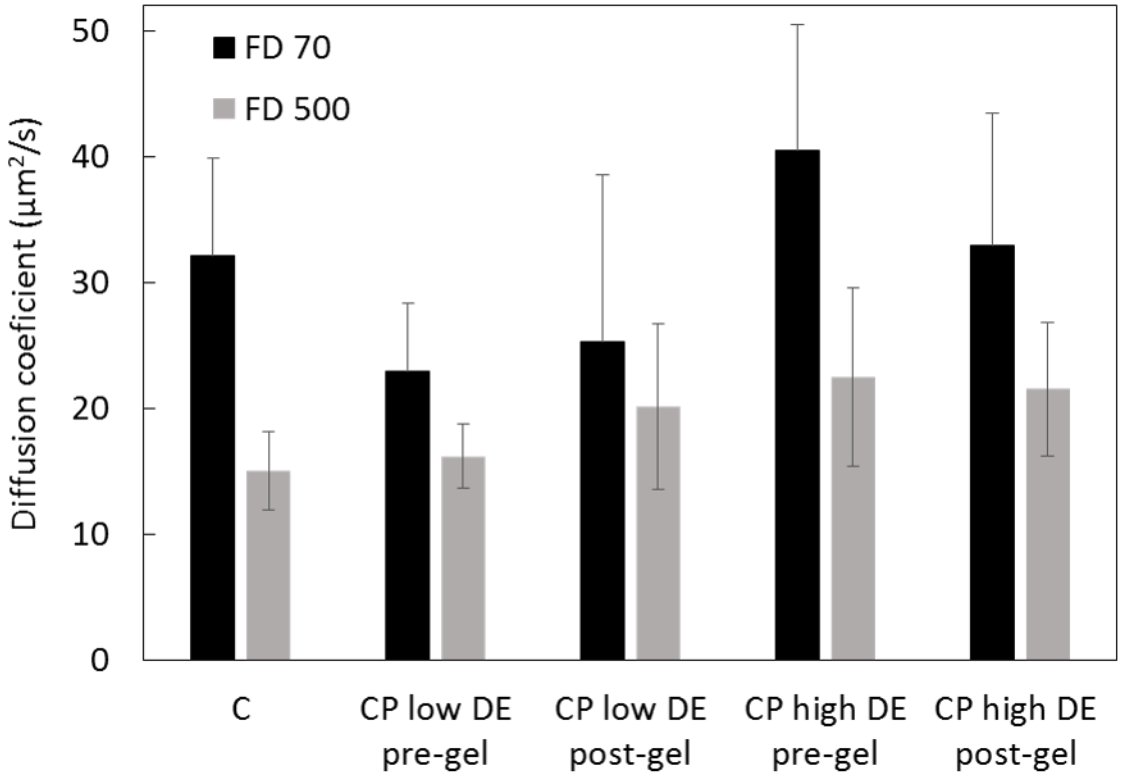

Figure 6. Diffusion coefficients of fluorescein isothiocyanate labelled dextran probes, FD 70 (r_H=8.0 ± 0.5 nm) and FD 500 (r_H=13.5 ± 1.1), in cellulose hydrogels containing Ca^{2+}-pectate gels assembled before or after cellulose synthesis.

Conclusions

It has been demonstrated that Ca^{2+}-pectate plays a key role in the load-bearing ability (under compression) of simplified plant cell wall models based on cellulose hydrogels. Order of polysaccharide assembly, i.e. pectin gel network formation prior to or after cellulose synthesis, impacts the resulting mechanical properties, including permeability, due to i) the

effects of the pectin-calcium gel on cellulose architecture, at all length scales, during cellulose deposition; and ii) microstructural homogeneity of the pectin-calcium gels. Direct molecular interaction between pectins and cellulose microfibrils is indicated from small angle scattering, but only when pectin is present during cellulose synthesis. The extent of the contribution to the mechanical and diffusion properties depends on the pectin degree of methylesterification, due to the strength and viscoelasticity of the formed Ca^{2+}-pectates. The results highlight the importance of the order of assembly of polysaccharides for cellulose composite hydrogels. Furthermore, although it should be considered that in plant cell walls other polysaccharides (hemicelluloses) are also present, our results provide insights into the potential contribution of pectin to cell wall mechanics.

Supporting information

Neutron and X-ray scattering length densities for cellulose and pectin. Two dimensional SANS patterns for the hydrogel samples soaked in D2O. Two dimensional scattering pattern for the CP low DE pre-gel showing the sector average applied to obtain the intensity in the equatorial (black lines) and meridional (red lines) directions. Parameters obtained from the SANS fits of the power-law plus core-shell cylinder with polydisperse radius model for the pure cellulose and the washed cellulose/pectin hydrogels.

Acknowledgements

The authors would like to thank Robert den Hollander, Tomer Rajsbaum and Marine Pellan for technical assistance with rheological measurements. David Appleton is acknowledged for performing calcium analysis and Roshan Cheetamun for monosaccharides and uronic acid analysis. Herbstreith & Fox KG is acknowledged for kindly providing the pectins. Erich Schuster is acknowledged for his help in setting up FRAP measurements. Professor Tony Bacic is gratefully acknowledged for reviewing the manuscript. We acknowledge the support

of a grant from the Australian Research Council (ARC) to the ARC Centre of Excellence in Plant Cell Walls [CE110001007].

References

Atmodjo, M. A., Hao, Z. Y., & Mohnen, D. (2013). Evolving Views of Pectin Biosynthesis. *Annual Review of Plant Biology, 64*, 747-779.

Bonilla, M. R., Lopez-Sanchez, P., Gidley, M. J., & Stokes, J. R. (2016). Micromechanical model of biphasic biomaterials with internal adhesion: Application to nanocellulose hydrogel composites. *Acta Biomater, 29*, 149-160.

Chanliaud, E., Burrows, K. M., Jeronimidis, G., & Gidley, M. J. (2002). Mechanical properties of primary plant cell wall analogues. *Planta, 215*(6), 989-996.

Chanliaud, E., & Gidley, M. J. (1999). In vitro synthesis and properties of pectin/acetobacter xylinus cellulose composites. *Plant Journal, 20*(1), 25-35.

Clark, A. H., & Farrer, D. B. (1996). Shear modulus-concentration relationships for low DE pectin calcium gels in the temperature range 20-85°C. *Food Hydrocolloids, 10*, 31-39.

Filisetti-Cozzi, T. M., & Carpita, N. C. (1991). Measurement of uronic acids without interference from neutral sugars *Analytical Biochemistry, 197*(1), 157-162.

Gidley, M. J., Morris, E. R., Murray, E. J., Powell, D. A., & Rees, D. A. (1979). Spectroscopic and stoichiometric characterisation of the calcium mediated association of pectate chains in gels and in the solid state. *Journal of the Chemical Society D, 22*, 990-992.

Gilbert, E. P., Schulz, J. C., & Noakes, T. J. (2006). 'Quokka' - the small-angle neutron scattering instrument at OPAL. *Phys. B (Amsterdam, Neth.), 385-86*, 1180-1182.

Grant, G. T., Morris, E. R., Rees, D. A., Smith, P. J. C., & Thom, D. (1973). Biological interactions between polysaccharides and divalent cations: The egg-box model. *FEBS Letters, 32*(1), 195:198.

Kline, S. R. (2006). Reduction and analysis of SANS and USANS data using IGOR Pro. *Journal of Applied Crystallography, 39*, 895-900.

Lin, D., Lopez-Sanchez, P., & Gidley, M. J. (2015). Binding of arabinan or galactan during cellulose synthesis is extensive and reversible. *Carbohydrate Polymers, 126*, 108-121.

Lin, D., Lopez-Sanchez, P., & Gidley, M. J. (2016). Interactions of pectins with cellulose during its synthesis in the absence of calcium. *Food Hydrocolloids, 52*, 57-68.

Lopez-Sanchez, P., Cersosimo, J., Wang, D. J., Flanagan, B., Stokes, J. R., & Gidley, M. J. (2015). Poroelastic Mechanical Effects of Hemicelluloses on Cellulosic Hydrogels under Compression. *Plos One, 10*(3), 1-19.

Lopez-Sanchez, P., Martinez-Sanz, M., Bonilla, M. R., Wang, D., Walsh, C. T., Gilbert, E. P., Stokes, J. R., & Gidley, M. J. (2016). Pectin impacts cellulose fibre architecture and hydrogel mechanics in the absence of calcium. *Carbohydr. Polym, 153* 236-245.

Lopez-Sanchez, P., Rincon, M., Wang, D., Brulhart, S., Stokes, J. R., & Gidley, M. J. (2014). Micromechanics and Poroelasticity of Hydrated Cellulose Networks. *Biomacromolecules, 15*(6), 2274-2284.

Lopez-Sanchez, P., Schuster, E., Wang, D., Gidley, M. J., & Strom, A. (2015). Diffusion of macromolecules in self-assembled cellulose/hemicellulose hydrogels. *Soft Matter, 11*(20), 4002-4010.

Martinez-Sanz, M., Gidley, M. J., & Gilbert, E. P. (2015). Hierarchical architecture of bacterial cellulose and composite plant cell wall polysaccharide hydrogels using small angle neutron scattering. *Soft Matter, 12*, 1534-1549.

Martinez-Sanz, M., Lopez-Sanchez, P., Gidley, M. J., & Gilbert, E. P. (2015). Evidence for differential interaction mechanism of plant cell wall matrix polysaccharides in hierarchically-structured bacterial cellulose. *Cellulose, 22*(3), 1541-1563.

Martinez-Sanz, M., Mikkelsen, D., Flanagan, B., Gidley, M. J., & Gilbert, E. P. (2016). Multi-scale model for the hierarchical architecture of native cellulose hydrogels. *Carbohydrate Polymers, 147*, 542-555.
Park, Y. B., & Cosgrove, D. J. (2012). Changes in Cell Wall Biomechanical Properties in the Xyloglucan-Deficient xxt1/xxt2 Mutant of Arabidopsis. *Plant Physiol., 158*(1), 465-475.
Peaucelle, A., Braybrook, S., & Hofte, H. (2012). Cell wall mechanics and growth control in plants: the role of pectins revisited. *Front. Plant Sci, 3*, 1-6.
Pettolino, F. A., Walsh, C., Fincher, G. B., & Bacic, A. (2012). Determining the polysaccharide composition of plant cell walls. *Nat. Protoc., 7*(9), 1590-1607.
Schuster, E., Eckardt, J., Hermansson, A. M., Larsson, A., Loren, N., Altskar, A., & Strom, A. (2014). Microstructural, mechanical and mass transport properties of isotropic and capillary alginate gels. *Soft Matter, 10*(2), 357-366.
Shedletzky, E., Shmuel, M., Trainin, T., Kalman, S., & Delmer, D. (1992). Cell-wall structure in cells adapted to growth on the cellulose-synthesis inhibitor 2,6-dichlorobenxonitrile- a comparison between 2 dicotyledoneous plants and a graminaceous monocot. *Plant Physiology, 100*(1), 120-130.
Skotheim, J. M., & Mahadevan, L. (2005). Physical limits and design principles for plant and fungal movements. *Science, 308*(5726), 1308-1310.
Somerville, C., Bauer, S., Brininstool, G., Facette, M., Hamann, T., Milne, J., Osborne, E., Paredez, A., Persson, S., Raab, T., Vorwerk, S., & Youngs, H. (2004). Toward a systems approach to understanding plant-cell walls. *Science, 306*(5705), 2206-2211.
Strom, A., Ribelles, P., Lundin , L., Norton, I., Morris, E. R., & Williams, M. A. K. (2007). Influence of pectin fine structure on the mechanical properties of calcium-pectin and acid-pectin gels. *Biomacromolecules, 8*, 2668-2674.
Wang, T., Park, Y. B., Cosgrove, D. J., & Hong, M. (2015). Cellulose-Pectin Spatial Contacts Are Inherent to Never-Dried Arabidopsis Primary Cell Walls: Evidence from Solid-State Nuclear Magnetic Resonance. *Plant Physiology, 168*(3), 871-884.
Wang, T., Zabotina, O., & Hong, M. (2012). Pectin-Cellulose Interactions in the Arabidopsis Primary Cell Wall from Two-Dimensional Magic-Angle-Spinning Solid-State Nuclear Magnetic Resonance. *Biochemistry, 51*(49), 9846-9856.
Whitney, S. E. C., Brigham, J. E., Darke, A. H., Reid, J. S. G., & Gidley, M. J. (1995). In-vitro assembly of cellullose/xyloglucan networks-ultrastructural and molecular aspects *Plant Journal, 8*(4), 491-504.
Zykwinska, A., Gaillard, C., Buleon, A., Pontoire, B., Garnier, C., Thibault, J. F., & Ralet, M. C. (2007). Assessment of in vitro binding of isolated pectic domains to cellulose by adsorption isotherms, electron microscopy, and X-ray diffraction methods. *Biomacromolecules, 8*(1), 223-232.